Effect of Al doping on Structural and Magnetic Properties of Iron Oxide Thin Films Prepared by Sol-Gel Method

*Aseya Akbar, Saira Riaz and Shahzad Naseem

Centre of Excellence in Solid State Physics, University of the Punjab, Lahore 54590, Pakistan
saira.cssp@pu.edu.pk

ABSTRACT

Iron oxides are material of interest because of their use in spintronic devices including Magnetic Tunnel Junctions (MTJ) and Random Access Memories (RAM). Among the various phases of iron oxide, Fe_2O_3 is the most stable form which shows antiferromagnetic or weak ferromagnetic behavior at room temperature. In order to enhance magnetic properties of Fe_2O_3, we here report the structural and magnetic properties of aluminum (Al) doped Fe_2O_3 thin films prepared using sol-gel method. Effect of aluminum doping on Fe_2O_3 thin films have been given very little consideration in the past particularly the reports on magnetic properties are limited. The presence of (012), (110), (006), (202), (024), (214) and (217) planes indicate the formation of pure hematite phase. No peaks corresponding to aluminum or aluminum oxide are observed. The undoped hematite thin films show ferromagnetic behavior as opposed to antiferromagnetic nature of bulk hematite. In case of hematite, spins in the adjacent planes are ferromagnetically coupled whereas, antiferromagnetic coupling arises with the spins of the adjacent planes. Spin orbit coupling between the two adjacent planes give rise to uncompensated spins of Fe^{3+} cations. Remarkable increase in magnetic moment is observed with the increase in dopant concentration.

1. INTRODUCTION

Transition metal oxides demonstrate variety of remarkable properties that can be used for spintronics, magnetic storage, photonic devices and for biomedical applications. But synthesis of transition metal oxides is complex as, transition metal oxides exhibit different stoichiometric forms (Garcia 2013). Among transition metal oxides, iron oxide is a promising candidate due to its high chemical and thermal stability. Iron oxide exists in three important crystallographic phases namely magnetite (Fe_3O_4), maghemite (γ-Fe_2O_3) and hematite (α-Fe_2O_3) (Riaz 2014, Riaz, 2013, Akbar 2014(a)). Among these phases hematite, α-Fe_2O_3, is a promising candidate owing to its wide applications as a catalyst, optical and magnetic devices and most importantly in spintronic devices including magnetic tunnel junctions, spin transistors etc. (Akbar

2014)

α-Fe_2O_3 posses rhombohedral structure belonging to R3c space group. Its unit cell can be described in two ways: (1) Rhombohedral unit cell: with two formula units and a=b=c=5.43Å and α ; (2) Hexagonal unit cell: with six formula units and a= 5.03Å and c=13.75Å (Rivera 2012). The lattice of α-Fe_2O_3 is composed of hexagonal closed arrays of oxygen anions. Every fourth out of six sites around oxygen anion are occupied by iron cation (Rivera 2012).

Hematite is antiferromagnetic in nature with Neel temperature of 960K (Glasscock 2008, Yogi 2013). It has a band gap of 2.2eV. Below temperature of 260K, it shows transition from antiferromagnetic to weak ferromagnetic behavior. This transition in magnetic properties arises due to canting in magnetization of two sublattices. Due to spin orbit coupling, canting between two adjacent planes arises. This produces uncompensated magnetic moment of Fe^{3+} cations. Thus, weak ferromagnetic or canted ferromagnetic behavior arises in otherwise antiferromagnetic hematite. As the temperature is reduced below 260K, spin direction of (111) plane changes from in plane to out of plane. This results in completely parallel arrangement of spins in the same plane. Perfectly antiparallel coupling arises with the spins of adjacent planes below 260K thus, converting hematite from weak ferromagnetic to antiferromagnetic. This type of transition is known as Morin Transition (Varshney 2013)

In order to improve the magnetic properties of hematite, doping of various cations has been reported in literature including Co, Cr, Zn, Mg etc. (Varshney 2013, Lian 2012, Suresh 2012) based on the valence state as well as ionic radius. Trivalent cations are most important in this regard due to same valence state of the dopant cation. However, despite the advantages of same valence state, aluminum (Al) doped Fe_2O_3 is given very little consideration especially, studies regarding magnetic properties are limited.

In this paper, we report synthesis and structural and magnetic characterization of aluminum doped Fe_2O_3 thin films. The films are prepared using sol-gel method. The dopant concentration is varied as 1-9%. Undoped and doped iron oxide thin films show ferromagnetic behavior. Changes in structural and magnetic properties are correlated with dopant concentration.

2. EXPERIMENTAL DETAILS

For preparation of undoped iron oxide thin films, iron nitrate ($Fe(NO_3)_3.9H_2O$) was used as precursor. Water and ethylene glycol were used as solvents. Iron nitrate was dissolved in deionized water and stirred at room temperature. Ethylene glycol was added to the above solution and heated on hot plate at 60 C to obtain stable sol. The details of sol-gel synthesis are reported earlier (Akbar 2014(b)). For aluminum (Al) doped iron oxide thin films, aluminum nitrate ($Al(NO_3)_3.9H_2O$) was dissolved in DI water and appropriate amount was added drop wise to iron oxide sol. The dopant concentration was varied as 1-9wt% (1%, 3%, 5%, 7%, and 9%). Sols were spin coated on copper substrate and annealed at 300 C for 60mins. Before spin coating, copper substrates were etched using diluted HCl and rinsed repeatedly in deionized water. The substrates were then ultrasonicated in acetone and isopropyl alcohol for 10min and 15min (Asghar 2006 (a), (b)).

The films were characterized structurally using Bruker D8 Advance X-ray Diffractometer with CuKα radiations (λ . 406Å). For studying magnetic properties, Lakeshore's 7407 Vibrating Sample Magnetometer was used.

3. RESULTS AND DISCUSSION

Fig. 1 show XRD patterns for aluminum doped iron oxide thin films. The presence of diffraction peaks corresponding to (012), (110), (006), (202), (024), (214) and (217) planes indicate the formation of hematite (α-Fe_2O_3) phase (JCPDS card no. 87-1165). No peaks corresponding to aluminum or aluminum oxide were observed. However, peak positions shifted to slightly higher angles. This shift of peak positions to higher angles is due to smaller ionic radius of Al^{3+} (0.53Å) as compared to Fe^{3+} (0.69Å). The pure phase of XRD and shift of peak positions to higher angles imply that Al atoms effectively occupy the Fe sites.
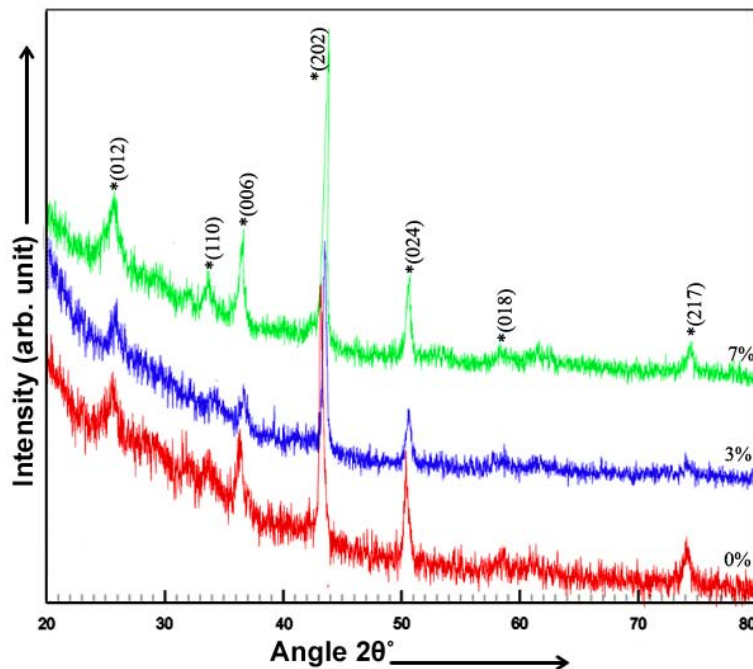
Fig. 1 XRD patterns for undoped and aluminum doped iron oxide thin films

Crystallite size (*t*), strain ($\Delta d/d$) and dislocation density (δ) (Cullity 1956) of aluminum doped iron oxide thin films is calculated using Eq. (1)-(3)

$$t = \frac{0.9\lambda}{B\cos\theta} \tag{1}$$

$$Strain = \frac{\Delta d}{d} = \frac{d_{\exp} - d_{pdf}}{d_{pdf}} \tag{2}$$

$$\delta = \frac{1}{t^2} \tag{3}$$

Where, λ is the wavelength (1.5406Å), B is the Full Width at Half Maximum (FWHM), d_{exp} is the d-spacing calculated from XRD pattern and d_{pdf} is the d-spacing taken from JCPDS card no. 87-1165. Fig. 2 (a) and (b) shows crystallite size, dislocation density and strain plotted as a function of dopant concentration. The crystallite size increases as the dopant concentration was increased to 5%. Further increase in dopant concentration resulted in decrease in crystallite size. This resulted to increase in dislocations in the films due to increase in number of grain boundaries. The grain growth in thin films depends on two important factors: (1) Neighboring grains that have different energies due to curvature of grain boundaries; (2) Stress in thin films (Riaz 2007). So, grain growth in Fe_2O_3 thin films increases as dopant concentration is increased to 5% due to reduced strain in thin films. At high dopant concentration, crystallite size decreased due to segregation of dopant at grain boundaries (Kuo 2006). The decrease in dislocations at low dopant concentration indicates that more and more Al atoms diffuses Fe_2O_3 lattice and reduces dislocations in films. All Al atoms settle in films dislocations and thus reduce the stresses (Jeetendra 2014) in the films as can be seen in Fig. 2(b).
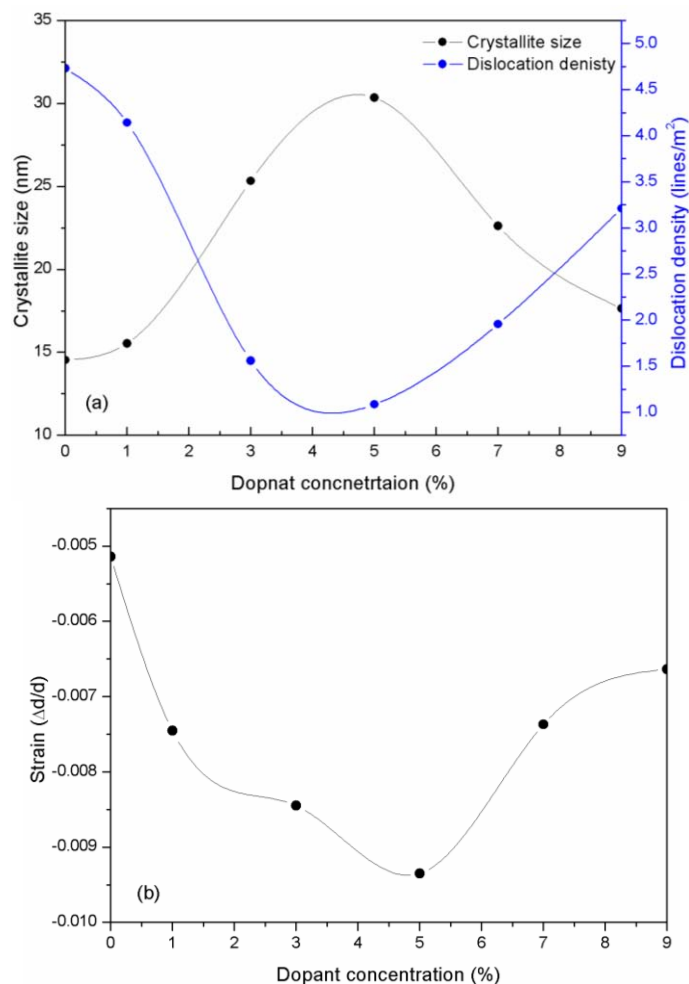
Fig. 2 (a) Crystallite size, dislocation density (b) Strain as a function of dopant concentration

Lattice parameters (a,c), x-ray density (ρ) and porosity of aluminum doped Fe_2O_3 thin films is calculated using Eq. (4)-(6).

$$\sin^2 \theta = \frac{\lambda^2}{3a^2}\left(h^2 + k^2 + hk\right) + \frac{\lambda^2 l^2}{4c^2} \tag{4}$$

$$\rho = \frac{1.66042\ \Sigma A}{V} \tag{5}$$

$$Porosity(\%) = \left[1 - \frac{\rho_{exp}}{\rho_{std}}\right] \times 100 \tag{6}$$

Where, *(hkl)* represent the miller indices, ΣA is the sum of atomic weights of the atoms in the unit cell, V is the volume of unit cell ($V=0.866a^2c$), ρ_{exp} is the experimental density (calculated using Eq. (5)), ρ_{std} is bulk density of iron oxide. Lattice parameters a and c of iron oxide thin films decreased as the dopant concentration is increased. The decrease in lattice parameters and unit cell volume is due to smaller ionic radius of aluminum as compared to that of iron thus leading to contraction in unit cell as can be seen in Fig. 3(b). Decreased unit cell then lead to increase in density. High density (5.2-5.8g/cm^3) and low porosity (4.3-11%) for the entire concentration range studied indicate the compact structure.
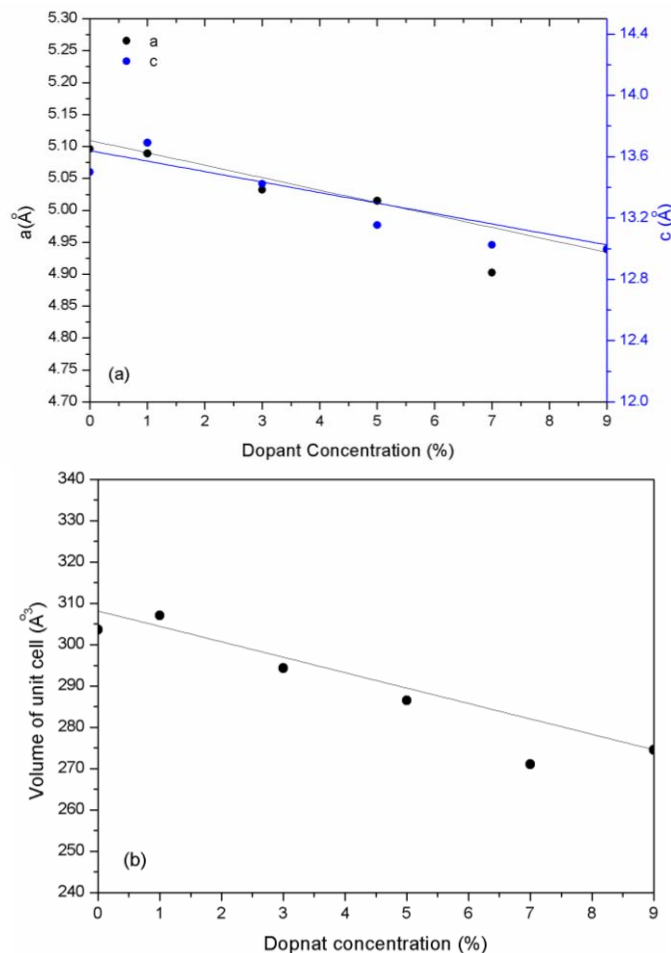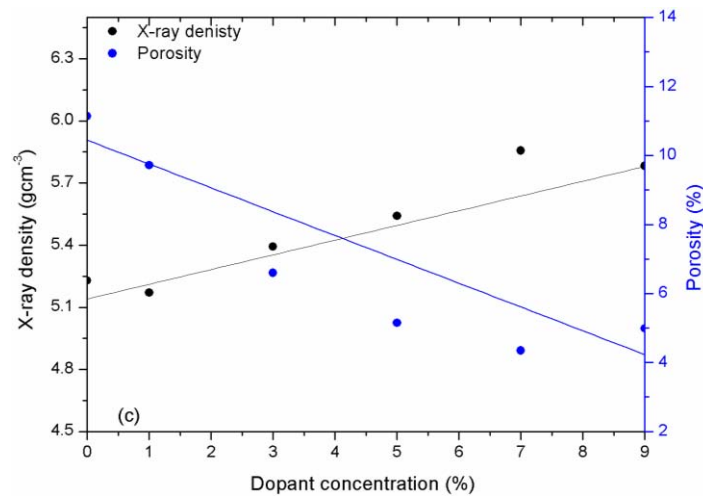
Fig. 3 (a) Lattice parameter (b) unit cell volume (c) x-ray density and porosity of Al doped Fe_2O_3 thin films as a function of dopant concentration
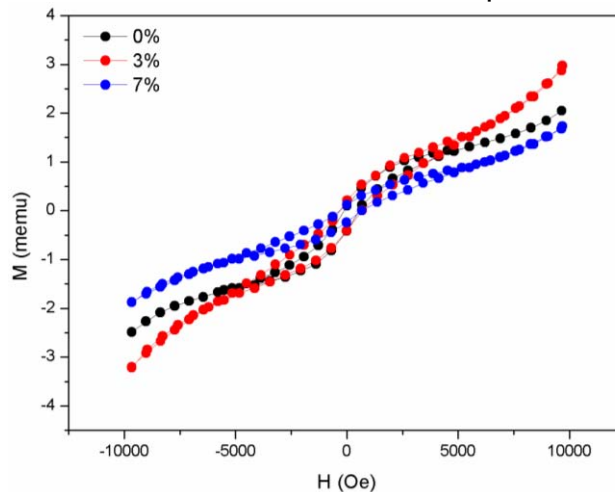
Fig. 4 M-H curves for Al doped Fe_2O_3 thin films

M-H curves for Al doped iron oxide thin films can be seen in Fig. 4. Saturation magnetization and coercivity are plotted as a function of dopant concentration in Fig. 5. Undoped Fe_2O_3 thin films exhibit ferromagnetic behavior. Undoped and Al doped hematite thin films show ferromagnetic behavior as opposed to antiferromagnetic nature of bulk hematite. In case of hematite, the spins in the same plane are arranged in parallel manner. Spins in adjacent planes are aligned antiparallel to each other. Antiferromagnetic coupling arises with the spins of the adjacent planes. Spin orbit coupling between the two adjacent planes give rise to uncompensated spins of Fe^{3+} cations (Akbar 2014, Rivera 2012). These uncompensated spins (Riaz 2011) produce the canting of spins between the planes. This is the cause of ferromagnetic behavior in otherwise antiferromagnetic material. As aluminum is incorporated in Fe_2O_3 lattice, canting of spin structure increased due to imbalance created by presence of aluminum in host lattice. This resulted in increase in saturation magnetization with increase in dopant concentration up to 5%. As the dopant concentration was increased beyond 5%

large number of defects including increased dislocations (as was seen in Fig. 2(a)) leads to inadequate alignment of spins. This resulted in less canting of spins thus, decreasing the saturation magnetization as can be seen in Fig. 5.
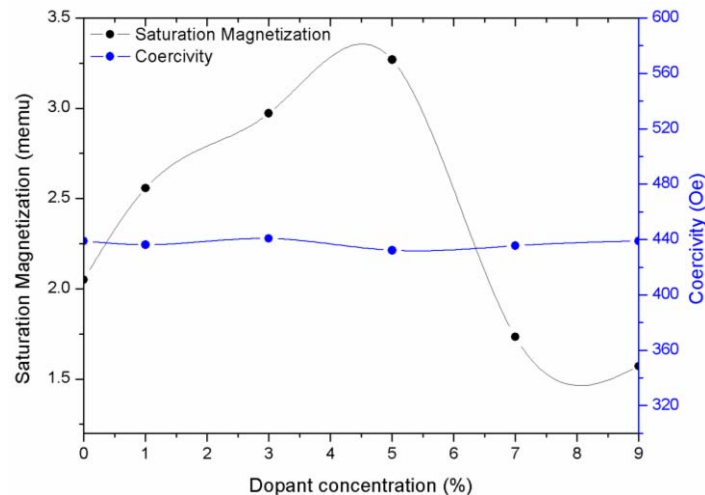
Fig. 5 Saturation magnetization and coercivity as a function of dopant concentration

4. CONCLUSIONS

Undoped and Al doped Fe_2O_3 thin films were deposited using sol-gel method. The dopant concentration was varied as 1%, 3%, 5%, 7% and 9%. XRD results indicated the formation of phase pure α-Fe_2O_3. No peaks corresponding to aluminum or aluminum oxide were observed indicating the successful replacement of Fe with Al. Undoped and Al doped α-Fe_2O_3 thin films show ferromagnetic behavior. Saturation magnetization increases as the dopant concentration is increased to 5%. Further increase in dopant concentration resulted in reduced magnetic properties.

REFERENCES

Akbar, A., Riaz, S., Bashir, M. and Naseem, S. (2014(a)), "Effect of Fe^{3+}/Fe^{2+} ratio on superparamagnetic behaviour of spin coated Iron oxide thin films," *IEEE Trans. Magn.*, doi: 10.1109/TMAG.2014.2312972.

Akbar, A., Riaz, S., Ashraf, R. and Naseem, S. (2014(b)), "Magnetic and magnetization properties of Co-doped Fe_2O_3 thin films," *IEEE Trans. Magn.*, doi: 10.1109/TMAG.2014.2311826

Asghar, M.H., Placido, F. and Naseem, S. (2006(a)), "Characterization of reactively evaporated TiO_2 thin films as high and medium index layers for optical applications," *Eur. Phys. J. - Appl. Phys.*, **35**, 177-184.

Asghar, M.H., Placido, F. and Naseem, S. (2006(a)), "Characterization of Ta2O thin films prepared by reactive evaporation," *Eur. Phys. J. - Appl. Phys.*, **36**, 119-124.

Cullity, B.D. (9 6), "Elements of x-ray diffraction," Addison Wesley Publishing Company, USA.

Garcia, H.A., Melo Jr., R.P., Azevedo, A. and Araujo, C.B. (20 3), "Optical and structural characterization of iron oxide and cobalt oxide thin films at 800 nm," *Appl. Phys. B.*, **111**, 313-321

Glasscock, J.A., Barnes, P.R.F., Plumb, I.C., Bendavid, A. and Martin, P.J. (2008), "Structural, optical and electrical properties of undoped polycrystalline hematite thin films produced using filtered arc deposition," *Thin Solid Films*, **516**, 1716-1724.

Jeetendra, S., Nagabhushana, H., Mrudula, K., Naveen, C.S., Raghu, P. and Mahesh, H.M. (20 4), "Concentration Dependent Optical and Structural Properties of Mo doped ZnTe Thin Films Prepared by e-beam Evaporation Method," *Int. J. Electrochem. Sci.,* **9**, 2944 – 2954

Kuo, S.Y., Chen, W.C., Lai, F.I., Cheng, C.P., Kuod, H.C., Wang, S.C. and Hsieh, W.F. (2006), "Effects of doping concentration and annealing temperature on properties of highly-oriented Al-doped ZnO films," *J Crystal Growth*, **287**, 78–84

Lian, X., Yang, X., Liu, S., Xu, Y., Jiang, C., Chen, J. and Wang, R. (20 2), "Enhanced photoelectrochemical performance of Ti-doped hematite thin films prepared by the sol–gel method," *Appl. Surf. Sci.*, **258**, 2307– 2311

Riaz, S. and Naseem , S., Xu, Y.B. (20   ), "Room temperature ferromagnetism in sol–gel deposited un-doped ZnO films," *J. Sol-Gel Sci. Technol.*, **59**, 584–590

Riaz, S. and Naseem, S. (2007), "Effect of reaction temperature and time on the structural properties of $Cu(In,Ga)Se_2$ thin films deposited by sequential elemental layer technique," *J. Mater. Sci. Technol.*, **23**, 499-503

Riaz, S., Akbar, A. and Naseem, S. (20 3), "structural, electrical and magnetic properties of iron oxide thin films," *Adv. Sci. Lett.*, **19**, 828-833.

Riaz, S., Akbar, A. and Naseem, S. (20 4), "Controlled nanostructuring of multiphase core-shell iron oxide nanoparticles," *IEEE Trans. Magn.*, **50**, 2300204

Rivera, R., Pinto, H.P., Stashans, A. and Piedra, L. (20 2), "Density functional theory study of Al-doped hematite," *Phys. Scr.*, 85, 015602

Suresh, R., Prabu, R., Vijayaraj, A., Giribabu, K., Stephen, A. and Narayanan, V. (20 2), "Facile synthesis of cobalt doped hematite nanospheres: Magnetic and their electrochemical sensing properties," *Mater. Chem. Phys.*, **134**, 590-596

Valdes, A.H., Zarate, R.A., Martinez, A.I., Canul, M.I.P., Lobato, M.A.G. and Villaroel, R. (20 4), "The role of solvents on the physical properties of sprayed iron oxide films," *Vacuum*, **105,** 26-32

Varshney, D. andYogi, A. (20 3), "Influence of Cr and Mn substitution on the structural and spectroscopic properties of doped hematite: $\alpha\text{-}Fe_{2-x}M_xO_3$ (0.0≤x≤0.50)," *J. Molecular Structure*, **1052**, 105–111

Yogi, A. and Varshney, D. (20 3), "Magnetic and structural properties of pure and Cr-doped hematite: $\alpha\text{-}Fe_{2-x}Cr_xO_3$ ($0 \leq x \leq 1$)," *J. Adv. Ceram.*, **2**, 360-369